JOURNAL OF OPTOELECTRONICS AND ADVANCED MATERIALS Vol. 10, No. 7, July 2008, p.1823 - 1827

Analysis of a Vector Hysteresis Measurement System

M. KUCZMANN
Laboratory of Electromagnetic Fields, Department of Telecommunications, Széchenyi István University, H-9026, Győr, Hungary

The paper deals with the numerical analysis of a vector hysteresis measurement system which is now under construction. The measurement set up consists of an induction motor which rotor has been removed, and its windings have been replaced to a special two phase one which can generate homogeneous magnetic field inside the motor. A round shaped specimen can be inserted into the arrangement. The two orthogonal components of the magnetic field intensity and of the magnetic flux density vectors can be measured by *H*-coils and *B*-coils, respectively. The Finite Element Method (FEM) with the $\boldsymbol{T}, \Phi - \Phi$ potential formulation has been applied in the simulations. The vector hysteresis property of the specimen has been approximated by the vector Preisach model, finally the nonlinear problem has been solved by the convergent fixed point technique. The aim of the present work is to focus on the design aspects of this kind of measurement system.

(Received April 1, 2008; accepted June 30, 2008)

Keywords: Vector hysteresis measurements, Vector Preisach model, nonlinear FEM

1. Introduction

The RRSST (Rotational Round shaped Single Sheet Tester) system is one of the possible measurement arrangements of the two dimensional vector hysteresis properties. In this case, the specimen has round shape, and consequently it can be put inside a rearranged induction motor. The other is to use square shaped specimen (RSSST) or hexagonal shaped specimen with special yoke. There are many other, but not commonly used measurement set up. First, the RRSST system has been analyzed, because the yoke is very cheap and it is easy to get [3,4]. The aim of this paper is to study the behavior of this measurement set up by applying a FEM procedure connected with the vector Preisach model of hysteresis [2,5].

2. The measurement set up

The block diagram of the two dimensional vector hysteresis measurement set up can be seen in Fig. 1. The RRSST system is an induction motor which rotor has been removed and the round shaped specimen has been installed in this place. The magnetic field inside the specimen can be generated by a special two phase winding which can be studied in Fig. 2. The two orthogonal components of the magnetic field intensity or of the magnetic flux density can be controlled by two independent current generators and the waveform of currents $i_x(t)$ and $i_y(t)$ can be set by a PC. The two orthogonal components of the magnetic field intensity vector and of the magnetic flux density vector inside the specimen can be measured by a sensor system. The tangential component of the magnetic field intensity can be measured by a coil placed onto the surface of the specimen (*H*-coils), the magnetic flux density inside the specimen can be measured by a coil slipped into holes of the specimen (*B*-coils). The magnetic field intensity can be measured by Hall sensors as well. These four signals can be measured by a NI-DAQ card (National Instruments Data Acquisition Card) installed on the PC, and a LabVIEW based software controls the measurements.

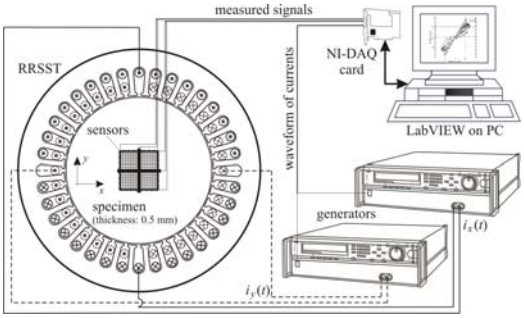

Fig. 1. The block diagram of the measurement system

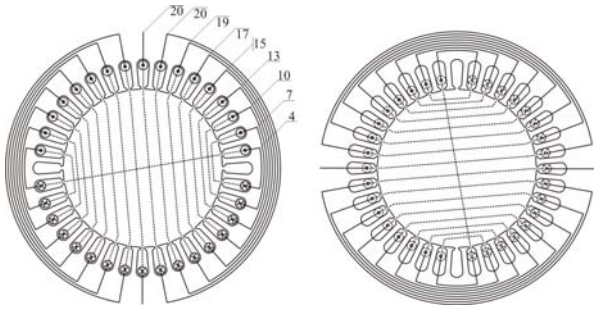

Fig. 2. The special two phase winding to generate a magnetic field specified by two orthogonal components

3. Governing equations

The measurement system presented in Section 2 can be efficiently simulated by FEM [1]. The stator core is made of laminated iron that is why the eddy currents have been neglected there. Eddy currents have been taken into account only in the specimen. According to the preliminary studies of the problem, the magnetic field intensity is much smaller inside the stator core than inside the specimen, so a linear characteristic has been supposed inside the stator core, and a nonlinear hysteretic one inside the specimen. The hysteresis characteristic of the material has been simulated by the vector Preisach model [2,5].

The Maxwell's equations in the eddy current free region Ω_n are as follows:

$$\nabla \times \boldsymbol{H} = \boldsymbol{J}_0,\ \nabla \cdot \boldsymbol{B} = 0,\ \boldsymbol{B} = \mu \boldsymbol{H}\ ,\text{in}\ \Omega_n\ ,(1)$$

where $\boldsymbol{H}$, $\boldsymbol{B}$, $\boldsymbol{J}_0$ and μ are the magnetic field intensity, the magnetic flux density, the excitation current density and the permeability, respectively, moreover $\mu = \mu_0$ in air and $\mu = 4000\mu_0$ in the stator core (μ_0 is the permeability of vacuum). The following Maxwell's equations have been used inside the specimen Ω_c:

$$\nabla \times \boldsymbol{H} = \sigma \boldsymbol{E},\ \nabla \times \boldsymbol{E} = -\partial \boldsymbol{B} / \partial t,\ \nabla \cdot \boldsymbol{B} = 0,\ \boldsymbol{B} = B\{\boldsymbol{H}\},\ \text{in}\ \Omega_c\ ,(2)$$

where $\boldsymbol{H}$, $\boldsymbol{B}$, $\boldsymbol{E}$, σ and $B\{\cdot\}$ are the magnetic field intensity, the magnetic flux density, the electric field intensity, the conductivity and the hysteresis operator. The vector hysteresis property of the magnetic material has been represented by the vector Preisach model.

The nonlinear and hysteretic relationship between the magnetic field intensity vector and the magnetic flux density vector has been handled by the polarization method as [6]

$$\boldsymbol{B} = B\{\boldsymbol{H}\} = \mu_{FP}\boldsymbol{H} + \boldsymbol{R}\ ,\text{in}\ \Omega_c\ ,(3)$$

where μ_{FP} is an optimal value of permeability, and $\boldsymbol{R}$ is the nonlinear residual term which can be calculated by an iterative technique based on the fixed point theorem. The value of μ_{FP} is usually selected as $\mu_{FP} = (\mu_{\max} + \mu_{\min})/2$ with the maximum and minimum slope of the characteristic, and it does not change during the fixed point based nonlinear iteration. The applied hysteresis characteristic in the x direction, the linear term $\mu_{FP}H_x$ and the nonlinear residual R_x can be seen in Fig. 3.

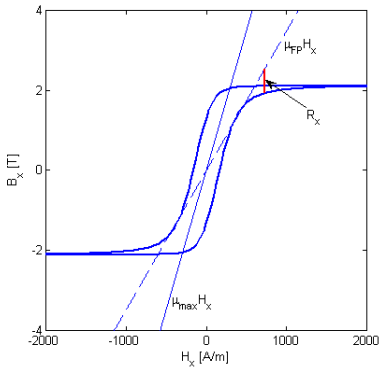

Fig. 3. The applied hysteresis curve and terms in (3)

In this model, the direct hysteresis model has been used which input is the magnetic field intensity vector. It can only be done if the so called $\boldsymbol{T}, \Phi - \Phi$ potential formulation is used [1]. The reduced scalar magnetic potential Φ can be applied in the eddy current free region Ω_n, and the current vector potential $\boldsymbol{T}$ with the reduced scalar potential Φ can be applied in the eddy current region Ω_c to represent the magnetic field intensity vector. The two regions must be coupled through the interface between them.

Starting from the solenoidal property of the excitation current density, an impressed field quantity $\boldsymbol{T}_0$ can be introduced to represent the excitation current, i.e.

$$\nabla \cdot \boldsymbol{J}_0 = 0\ \rightarrow\ \boldsymbol{J}_0 = \nabla \times \boldsymbol{T}_0\ ,(4)$$

which has been represented by vector shape functions associated to the edges of the FEM mesh, and $\boldsymbol{T}_0$ has been calculated by the Biot-Savart's law [7]. Substituting the representation in (4) into the first Maxwell's equation in (1) results in

$$\boldsymbol{H} = \boldsymbol{T}_0 - \nabla\Phi\ ,\text{in}\ \Omega_n\ .(5)$$

The solenoidal property of the magnetic flux density in (1) can be reformulated by the following partial differential equation:

$$\nabla \cdot \left(\mu\left[\boldsymbol{T}_0 - \nabla\Phi\right]\right) = 0\ ,\text{in}\ \Omega_n\ .(6)$$

The eddy current field $\sigma\boldsymbol{E}$ has also the solenoidal property, i.e. $\nabla \cdot (\sigma\boldsymbol{E}) = 0$, and it can be represented by the unknown current vector potential $\boldsymbol{T}$ as $\sigma\boldsymbol{E} = \nabla \times \boldsymbol{T}$, from which the electrical field intensity can be expressed as $\boldsymbol{E} = 1/\sigma\, \nabla \times \boldsymbol{T}$. Substituting the representation of $\sigma\boldsymbol{E}$ into the first Maxwell's equation in (2) results in $\boldsymbol{H} = \boldsymbol{T} - \nabla\Phi$, however the formulation

$$\boldsymbol{H} = \boldsymbol{T}_0 + \boldsymbol{T} - \nabla\Phi \text{ ,in } \quad \Omega_c \quad (7)$$

is usually applied, because then it is easier the coupling of the eddy current free problem to the eddy current one along the interface between the two regions [7]. Substituting this representation with the polarization formula of the magnetic flux density (3) into the second Maxwell's equation in (2) results in the nonlinear partial differential equation

$$\nabla\times\left(\frac{1}{\sigma}\nabla\times\boldsymbol{T}\right)-\nabla\left(\frac{1}{\sigma}\nabla\cdot\boldsymbol{T}\right)+\mu_{FP}\left(\frac{\partial\boldsymbol{T}_0}{\partial t}+\frac{\partial\boldsymbol{T}}{\partial t}-\nabla\frac{\partial\Phi}{\partial t}\right)+\frac{\partial\boldsymbol{R}}{\partial t}=\boldsymbol{0}, \text{ in } \Omega_c . \quad (8)$$

The second term in the above equation must be inserted as implicit Coulomb gauge enforcement to satisfy $\nabla\cdot\boldsymbol{T}=0$ [1]. The solenoidal property of the magnetic flux density in (2) can be written as

$$\nabla\cdot\left(\mu_{FP}\left[\boldsymbol{T}_0+\boldsymbol{T}-\nabla\Phi\right]+\boldsymbol{R}\right)=0 \text{ ,in } \Omega_c . \quad (9)$$

The partial differential equation (6) in the air region and in the stator core, moreover the nonlinear partial differential equations (8) and (9) are valid in the specimen. The two formulations must be coupled through the interface between the air region and the specimen. The tangential component of the magnetic field intensity and the normal component of the magnetic flux density must be continuous on this surface. This results in the Dirichlet type boundary condition $\boldsymbol{T}\times\boldsymbol{n}=\boldsymbol{0}$ [1]. Only the half of the arrangement has been analyzed because of symmetry along z=0 plane. Here $\boldsymbol{T}\cdot\boldsymbol{n}=0$ has been applied [1].

4. FEM formulation of the problem

The problem has been solved by FEM. The x-y plane of the arrangement has been discretized by triangular mesh (Fig. 4) which has been extruded in the z direction. The impressed field $\boldsymbol{T}_0$ has been represented by edge elements, the unknown potentials $\boldsymbol{T}$ and Φ have been approximated by nodal elements [1,7]. The x component of the Biot-Savart field can be seen in Fig. 5.

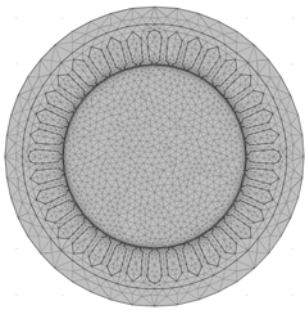

Fig. 4. The triangular mesh in the x-y plane.

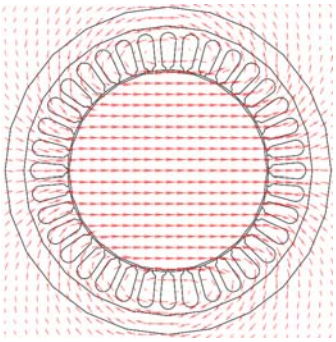

Fig. 5. The x component of Biot-Savart field

The weak formulation of the partial differential equations can be formulated by using the Galerkin form of the weighted residuals method,

$$\int_{\Omega_c}\frac{1}{\sigma}\nabla\times\boldsymbol{W}\cdot\nabla\times\boldsymbol{T}\,\mathrm{d}\Omega+\int_{\Omega_c}\frac{1}{\sigma}\nabla\cdot\boldsymbol{W}\,\nabla\cdot\boldsymbol{T}\,\mathrm{d}\Omega+\int_{\Omega_c}\mu_{FP}\boldsymbol{W}\cdot\left(\frac{\partial\boldsymbol{T}_0}{\partial t}+\frac{\partial\boldsymbol{T}}{\partial t}-\nabla\frac{\partial\Phi}{\partial t}\right)\mathrm{d}\Omega + \int_{\Omega_c}\boldsymbol{W}\cdot\frac{\partial\boldsymbol{R}}{\partial t}\,\mathrm{d}\Omega=0, \quad \text{in} \quad \Omega_c, \quad (10)$$

$$-\int_{\Omega_c}\mu_{FP}\nabla N\cdot\left(\frac{\partial\boldsymbol{T}_0}{\partial t}+\frac{\partial\boldsymbol{T}}{\partial t}-\nabla\frac{\partial\Phi}{\partial t}\right)\mathrm{d}\Omega-\int_{\Omega_c}\nabla N\cdot\frac{\partial\boldsymbol{R}}{\partial t}\,\mathrm{d}\Omega=0, \quad \text{in} \quad \Omega_c, \quad (11)$$

$$-\int_{\Omega_n}\mu\,\nabla N\cdot\left(\frac{\partial\boldsymbol{T}_0}{\partial t}-\nabla\frac{\partial\Phi}{\partial t}\right)\mathrm{d}\Omega=0, \quad \text{in} \quad \Omega_n. \quad (12)$$

Here $\boldsymbol{W}$ is the shape function of the unknown current vector potential $\boldsymbol{T}$, N is the shape function of the reduced scalar potential Φ. The time derivative of equations (9) and (6) must be taken because of symmetry of the resulting system of equations.

The system of the nonlinear ordinary differential equations (10)-(12) has been solved in the $(n+1)^{th}$ time step by the following scheme,

$$\frac{\boldsymbol{a}^{(n+1)}-\boldsymbol{a}^{(n)}}{\Delta t}=\vartheta\frac{\partial\boldsymbol{a}^{(n+1)}}{\partial t}+(1-\vartheta)\vartheta\frac{\partial\boldsymbol{a}^{(n)}}{\partial t}, \quad (13)$$

where Δt is the time stepping of the time discretization. This results in

$$\int_{\Omega_c}\frac{\Delta t}{\sigma}\nabla\times\boldsymbol{W}\cdot\left[\vartheta\nabla\times\boldsymbol{T}^{(n+1)}+(1-\vartheta)\nabla\times\boldsymbol{T}^{(n)}\right]\mathrm{d}\Omega+\int_{\Omega_c}\frac{\Delta t}{\sigma}\nabla\cdot\boldsymbol{W}\left[\vartheta\nabla\cdot\boldsymbol{T}^{(n+1)}+(1-\vartheta)\nabla\cdot\boldsymbol{T}^{(n)}\right]\mathrm{d}\Omega + \int_{\Omega_c}\mu_{FP}\boldsymbol{W}\cdot\left[\left(\boldsymbol{T}_0^{(n+1)}+\boldsymbol{T}^{(n+1)}-\nabla\Phi^{(n+1)}\right)-\left(\boldsymbol{T}_0^{(n)}+\boldsymbol{T}^{(n)}-\nabla\Phi^{(n)}\right)\right]\mathrm{d}\Omega + \int_{\Omega_c}\boldsymbol{W}\cdot\left[\boldsymbol{R}^{(n+1)}-\boldsymbol{R}^{(n)}\right]\mathrm{d}\Omega=0, \quad \text{in} \quad \Omega_c, \quad (14)$$

$$-\int_{\Omega_c}\mu_{FP}\nabla N\cdot\left[\left(\boldsymbol{T}_0^{(n+1)}+\boldsymbol{T}^{(n+1)}-\nabla\Phi^{(n+1)}\right)-\left(\boldsymbol{T}_0^{(n)}+\boldsymbol{T}^{(n)}-\nabla\Phi^{(n)}\right)\right]\mathrm{d}\Omega - \int_{\Omega_c}\nabla N\cdot\left[\boldsymbol{R}^{(n+1)}-\boldsymbol{R}^{(n)}\right]\mathrm{d}\Omega=0, \quad \text{in} \quad \Omega_c, \quad (15)$$

$$-\int_{\Omega_n}\mu\nabla N\cdot\left[\left(\boldsymbol{T}_0^{(n+1)}-\nabla\Phi^{(n+1)}\right)-\left(\boldsymbol{T}_0^{(n)}-\nabla\Phi^{(n)}\right)\right]\mathrm{d}\Omega=0,\quad\text{in}\quad\Omega_n. \tag{16}$$

In these studies $\vartheta=2/3$ has been used (Galerkin scheme).

The problem is nonlinear, which must be solved iteratively. The applied fixed point based algorithm is very simple:

1. Starting from demagnetized state, $\boldsymbol{H}=\boldsymbol{0}$, $\boldsymbol{B}=\boldsymbol{0}$. Calculate μ_{FP} using the x component of the vector hysteresis characteristics.
2. Solve the equations (14)-(16) in the time step (n+1).
3. Calculate the magnetic field intensity inside the specimen, $\boldsymbol{H}=\boldsymbol{T}_0+\boldsymbol{T}-\nabla\Phi$.
4. Calculate the magnetic flux density by the hysteresis model, $\boldsymbol{B}=B\{\boldsymbol{H}\}$.
5. Update the residual term $\boldsymbol{R}^{(n+1)}$ as $\boldsymbol{R}=\boldsymbol{B}-\mu_{FP}\boldsymbol{H}$.
6. Repeat from step 2 until convergence.

This procedure is convergent, but unfortunately it is very slow.

4. Numerical results

The independent excitation currents have been prescribed as $i_x(t)=I_x\sin(\omega t+\alpha)$, and $i_y(t)=I_y\sin(\omega t+\beta)$. The amplitude and the phase of currents define the polar angle and amplitude of the magnetic field intensity vector or the magnetic flux density vector. Controlling the flux or the magnetic field can be worked out by an iterative feedback algorithm which simulation is time consuming. Here the relationship between the currents and the magnetic field intensity is studied at $f=5\mathrm{Hz}$, $f=50\mathrm{Hz}$ and $f=500\mathrm{Hz}$. The conductivity of the specimen is $\sigma=2\cdot10^6\,\mathrm{S/m}$, the value of μ_{FP} is about $4000\mu_0$, and the peak value of currents is 1A. The thickness of the sample is 0.5 mm.

The FEM mesh consists of 94512 prism elements, the number of unknowns is 68893, and 5800 vector hysteresis models with 20 scalar models per one vector model, i.e. the full number of Preisach models is 116000.

Here, only counter clockwise rotation field is presented. The aim is to analyze the variation of the magnetic field inside the specimen and in the place where sensors are usually located.

The magnetic field intensity has been increased in the x direction than it rotates in the counter clockwise direction. The stationary state of the two orthogonal components of the magnetic field intensity at point x=y=z=0 can be seen in Fig. 5 and in Fig. 6. The effect of eddy currents can be sensed at $f=500\mathrm{Hz}$, however $f=50\mathrm{Hz}$ seems to be almost the same as the results of $f=5\mathrm{Hz}$ calculations. Fig. 8 and Fig. 9 show the time variation of the x and of the y components of the magnetic field intensity at some points inside the specimen ($f=50\mathrm{Hz}$). The coordinates are given in the legend of the figures in mm, and z=0. It can be concluded that the magnetic field intensity is almost homogeneous inside the specimen, however its behavior is very strange close to the boundary. It determines the size of B-coils, i.e. B-coils should not be as wide as the specimen.

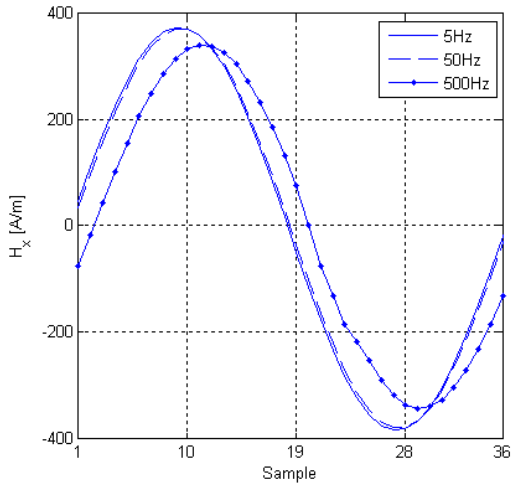

Fig. 6. Variation of x components of the magnetic field variation at x=y=z=0

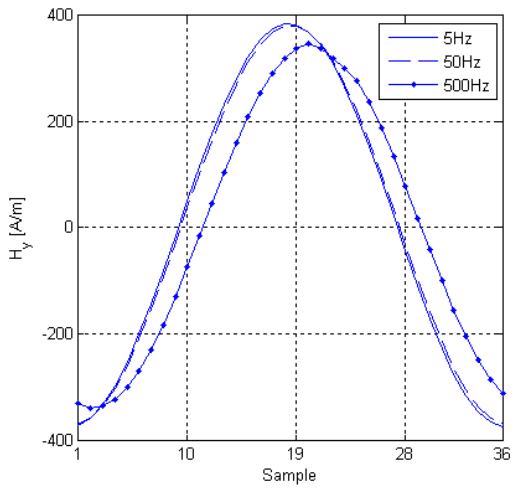

Fig. 7. Variation of y components of the magnetic field variation at x=y=z=0

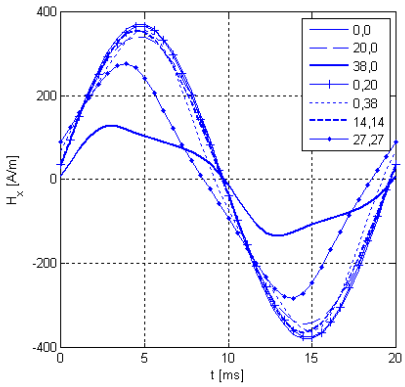

Fig. 8. Variation of x components of the magnetic field variation at some points

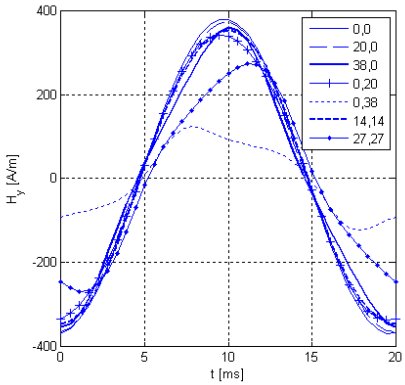

Fig. 9. Variation of y components of the magnetic field variation at some points

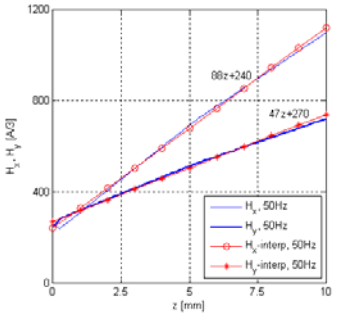

Fig. 10. The magnetic field intensity is increasing by increasing the distance between H-coil and the surface of Specimen.

The magnetic field intensity is increasing almost linearly measuring from the surface of the specimen where the *H*-coils are usually located. Fig. 10 shows this variation.

Applying more than one *H*-coil in every direction, the magnetic field intensity components on the surface of the specimen can be extrapolated.

5. Conclusions

The numerical analysis of a RRSST system has been shown in the paper. The FEM with the 2D vector Preisach model has been used for the simulations. The magnetic vector potential assumes an inverse vector hysteresis operator which is very slow in case of using the direct model in inverse mode as it was presented in [2]. The potential formulation used here enables the use of direct model which speeds up the algorithm. Aim of further research is to use a faster nonlinear solver (the Newton-Raphson scheme), and to analyze the effect of anisotropy. Finally numerical results must be compared with measured ones.

The problem has been solved by the help of functions of the commercial FEM solver COMSOL Multiphysics.

Acknowledgements

This paper was supported by the János Bolyai Research Scholarship of the Hungarian Academy of Sciences (BO/00064/06) and by Széchenyi István University (15-3002-51).

References

[1] O. Bíró, CAD in Electromagnetism, Comput. Meth. Appl. Mech. Engrg., 391, 1999.

[2] M. Kuczmann, Numerical Analysis of a 2D Vector Hysteresis Measurement System Under Construction, Journal of Electrical Engineering, vol.57, no.8/S, Bratislava, Slovakia , pp. 44-47, 2006.

[3] V. Gorican, A. Hamler, B. Hribernik, M. Jesenik, M. Trlep, Proceedings of the 6th International Workshop on 1&2-Dimensional Magnetic Measurement and Testing, 391, 2000.

[4] M. Kuczmann, P. Kis, A. Iványi, J. Füzi, Vector Hysteresis Measurement, Physica B, vol. 343, 2000, pp. 390-394.

[5] M. Kuczmann, A. Iványi, Identification of Isotropic and Anisotropic Vector Preisach Model, Preisach Memorial Book (ed.by A. Iványi), Akadémiai Kiadó, Budapest, 2005, pp. 89-102.

[6] Hantila, I. F., A Method For Solving Stationary Magnetic Field in Nonlinear Media, Rev. Roum. Sei. Techn. Elecirotechn. Et. Energ., vol. 20, 1975, pp. 397-407.

[7] Bíró, O. Edge Element Formulations of Eddy Current Problems, Comput. Meth. Appl. Mech. Engrg. Vol. 169, 1999, pp. 391–405.

*Corresponding author:Kuczmann@sze.hu